Phys. Med. Biol. 49 (2004) 2103–2115 PII: S0031-9155(04)74865-4

Reconstruction of action potential of repolarization in patients with congenital long-QT syndrome

Akihiko Kandori[1], Wataru Shimizu[2], Miki Yokokawa[2], Shiro Kamakura[2], Kunio Miyatake[2], Masahiro Murakami[3], Tsuyoshi Miyashita[1], Kuniomi Ogata[1] and Keiji Tsukada[4]

[1] Central Research Laboratory, Hitachi, Ltd, 1-280 Higashi-koigakubo, Kokubunji, Tokyo 185-8601, Japan
[2] National Cardiovascular Center, Osaka, Japan
[3] Hitachi High-technologies, Ibaraki, Japan
[4] Okayama University, Okayama, Japan

E-mail: kandori@rd.hitachi.co.jp

Received 19 January 2004
Published 4 May 2004
Online at stacks.iop.org/PMB/49/2103
DOI: 10.1088/0031-9155/49/10/019

Abstract

A method for reconstructing an action potential during the repolarization period was developed. This method uses a current distribution—plotted as a current-arrow map (CAM)—calculated using magnetocardiogram (MCG) signals. The current arrows are summarized during the QRS complex period and subtracted during the ST-T wave period in order to reconstruct the action-potential waveform. To ensure the similarity between a real action potential and the reconstructed action potential using CAM, a monophasic action potential (MAP) and an MCG of the same patient with type-I long-QT syndrome were measured. Although the MAP had one notch that was associated with early afterdepolarization (EAD), the reconstructed action potential had two large and small notches. The small notch timing agreed with the occurrence of the EAD in the MAP. On the other hand, the initiation time of an abnormal current distribution coincides with the appearance timing of the first large notch, and its end time coincides with that of the second small notch. These results suggest that a simple reconstruction method using a CAM based on MCG data can provide a similar action-potential waveform to a MAP waveform without having to introduce a catheter.

(Some figures in this article are in colour only in the electronic version)

1. Introduction

The action potential is a basic unit of electrical activation in the heart. It has a variety of waveforms depending on the atrial myocardium, the ventricular myocardium and the conduction pathways (AV node, His, bundle branches and Purkinje) (Hoffman and Cranefield 1960). To detect the action potential, monophasic action potential (MAP) recording has been used since the first comparison study between action potential and MAP was performed (Hoffman *et al* 1959). MAP recordings revealed afterdepolarizations during the late repolarization period in two patients with congenital long-QT syndrome (Gavrilescu and Luca 1978). Furthermore, an early afterdepolarization (EAD) was detected on a MAP of patients with idiopathic long-QT syndrome (Bonatti *et al* 1983). It has also been reported that the appearance of the EAD in the LQT group was associated with an increased amplitude of the late component of the TU complex and that the corrected QT (QTc) interval was prolonged by isoproterenol (Shimizu *et al* 1991). Moreover, it has been reported that the EAD triggered the ventricular premature complex (Shimizu *et al* 1994, 1995) and *torsades de pointes* in patients with long-QT syndrome (Kurita *et al* 1997, Vos *et al* 2000).

Electrical propagation of the ventricular action potential was studied using a one-dimensional Beeler–Reuter cable model (Beeler and Reuter 1977). The model has been used to reconstruct two-dimensional electrical propagation (Roberge *et al* 1986, Delgado *et al* 1990). These studies suggested that threshold requirements for active propagation were lower for transverse propagation than for longitudinal propagation, which is associated with a line of gap junctions. Although the model still has some problems (fibre orientation, three-dimensional complexity, etc, in the real heart), it is very useful for understanding the mechanism of electrical activation in the myocardial muscle.

The repolarization wave represents current flow which is originated from the potential difference of action potential mainly between endocardial and epicardial regions. Thus, a magnetocardiogram (MCG) can depict the potential derivative at each time point, i.e. the difference of action potential of two regions. The MCG has a high spatial resolution for cardiac electrical sources because it suffers little interference from various organs such as the bones and the lungs (Hosaka *et al* 1976, Cuffin 1978). Electrical distributions have been analysed mathematically by a multiple-source model (Karp *et al* 1980) and a realistic torso model (Nenonen *et al* 1991). To simplify the analysis, we have used a tangential vector calculated from the normal component of a magnetic field, because it reflects an electrically activated current distribution (Hosaka and Cohen 1976, Tsukada *et al* 1998, 1999, Miyashita *et al* 1998, Horigome *et al* 1999, Kandori *et al* 2001a, 2001b, 2002, Kanzaki *et al* 2003). In the visualization of a tangential vector, MCGs of adult patients with long-QT syndrome (LQTS) had an abnormal current distribution in the cases of LQT1 and LQT2 types (Kandori *et al* 2002).

In the present study, we developed a method that uses MCG signals to reconstruct an action potential in a repolarization phase. We then verified that this method can be used to estimate the presence of the EAD in LQTS patients.

2. Methods

2.1. Relationship between action potential and electrocardiogram

The relationship between a cell-membrane ionic current, an action potential in ventricular muscle and an electrocardiogram can be represented by figure 1. When the selectivity of the ions in the current increases, an ionic current occurs in accordance with the ionic potential

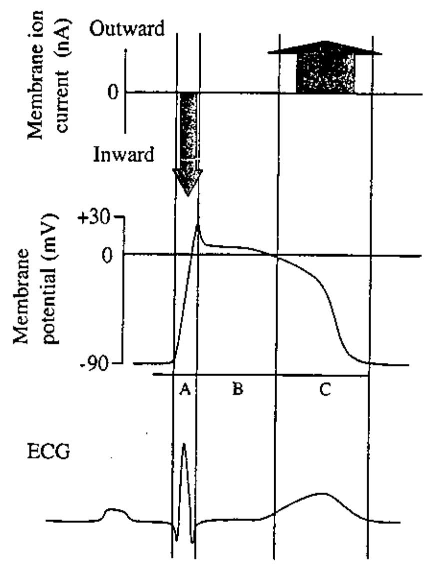

Figure 1. Relationship between cell-membrane ionic current, action potential and ECG signal.

slope. The slope is made by the difference in ionic densities inside and outside of the ventricular cell. Because the ionic flow can be considered as a current, it is called the cell-membrane ionic current. The main current has two types: inward current and outward current. In a short period of depolarization (A), a large inward current (from outside to inside the cell) flows. The representative inward current for Na^+ ions is I_N. After the depolarization, the status of the ventricular cell enters a refractory period (B). During the B period, the ionic current hardly flows. In the last repolarization period (C), the outward current (from inside to outside the cell) slowly flows. The typical outward current for K^+ ions is given as I_K. The current flow produces an action potential on the ventricular cell as shown in the middle figure. The total action potential then makes a voltage, which forms the electrocardiogram (ECG) as shown in the lower figure, on the living body surface. It has been considered that the ECG waveforms are formed by a differentiate voltage between the epicardium and the endocardium on the ventricular muscle, or they are formed by a derivative voltage (propagation of an electrical activity) between neighbouring cells. As a result, QRS complexes appear in the depolarization period (A), and T-waves are formed in the repolarization period (C). The model given in figure 1 is simplified so that the mechanism of electrical activation in the myocardial muscle can be understood more easily, although the other inward and outward currents have been found in previous studies.

We use a Beeler–Reuter model (Beeler and Reuter 1977) based on a cable network to represent the electrical propagation of the cell membrane as shown in figure 2, because an MCG waveform reflects a spatial electrical activation. In figure 2, three ventricular cells are used to represent a two-dimensional model of electrical propagation. The first electrical signal (V_0) in the model comes from the conduction system in the heart. When the V_0 inside the cell exceeds a threshold (about -60 mV), an ion-channel switch opens and a cell-membrane ionic current begins flowing as an inward current (i_{m1}). The occurrence of the flowing ions produces an action potential V_0 at position P_0. After the current starts to flow, a current (i_{i12}) at gap junction J_{01} (connected with two ventricular cells) also flows through a gap with resistance (r_{i12}), and the cell has a potential V_1. When the V_1 exceeds a threshold (about -60 mV), the ion-channel switch opens and a cell-membrane ionic current begins flowing as an inward current (i_{m2}). The inward current produces an action potential V_1 at position P_1. After flowing, a current (i_{i23}) at gap junction J_{12} also flows through a gap with resistance (r_{i23}), and the cell has a

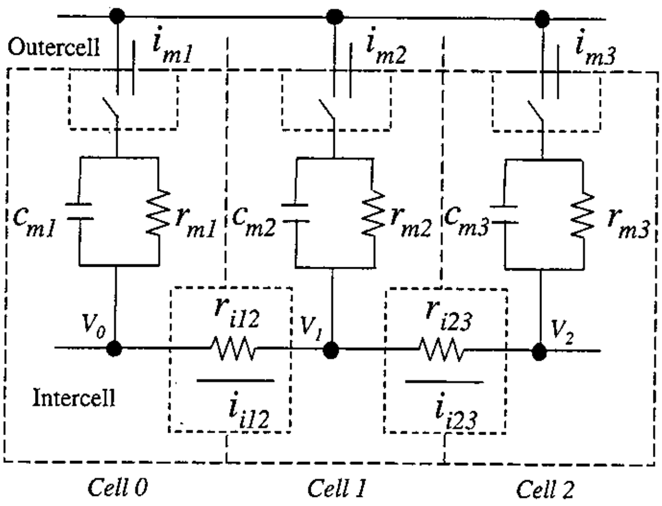

Figure 2. Equivalent circuit of an electrical propagation model for a myocardial cell-to-cell communication.

potential V_2 at position P_2. According to this cell model, the electrical activation propagates in the heart and each potential (V_1, V_2) waveform is formed. Here, it is considered that measured ECG and MCG signals are associated with the derivative waveforms of the formed potential depending on the current flow (i_{i12} and i_{i23} in some cells), because the measurement position is far from the source current. Under such a hypothesis, the current in the cells at one time is $i_{i12} = (V_1 - V_0)/r_{i12}$ or $i_{i23} = (V_2 - V_1)/r_{i23}$, and it reflects a differential potential between the two cells when the gap resistances are uniform in all ventricular cells. The currents during the activation time must be summed in order to calculate the action potential. The start time of the summation must be set within a non-activation period (i.e., the pQ period) in the heart, and the initial value of the summation at the start time must be zero.

In the above-mentioned method, we focus on a calculation in the depolarization period, in which an inward current flows. In contrast, we must subtract a current from the maximum summation value in order to calculate the action potential in the repolarization period, in which an outward current flows. It should be noted that the initial current of the repolarization is subtracted from the end value of the summation in the depolarization. The summation and subtraction of the current in the heart give an action-potential waveform.

2.2. A method for calculating action potential by using magnetocardiographic signals

A current-arrow map (CAM), which visualizes a pseudo current pattern in a heart, can be used to produce an activation current in the heart. The CAM is derived from the derivatives of the normal component (Bz) of the MCG signals (Hosaka and Cohen 1976, Miyashita *et al* 1998, Kandori *et al* 2001a, 2001b) as

$$Ix = \mathrm{d}Bz/\mathrm{d}y \tag{1}$$

and

$$Iy = -\mathrm{d}Bz/\mathrm{d}x. \tag{2}$$

The magnitude of the current arrows ($I = (Ix^2 + Iy^2)^{1/2}$) is shown as a contour map. The CAM directly provides a current pattern in the heart without having to solve a nonlinear inverse problem.

The method for calculating the action potential is shown in figures 3 and 4. Figure 3 visualizes the relationship between the action-potential waveform and the calculated current

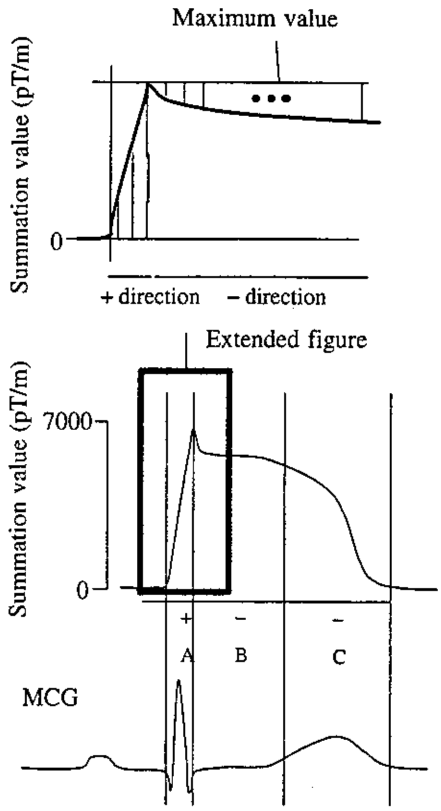

Figure 3. Block diagram for reconstructing an action potential.

arrows. The bottom figure in figure 3 indicates the MCG waveform, the middle figure indicates the reconstructed action-potential waveform and the top figure indicates the extended middle figure. In the top figure, current arrows are drawn so that the computation can be understood easily. The absolute value of the current arrows is added during the depolarization period (positive direction in the figure). At the end of the depolarization, the total value becomes a maximum. After determining the maximum value, the absolute value of the current arrows is subtracted during the repolarization period (negative direction in the figure).

Figure 4 shows the procedure for calculating the action potential. First, the CAM at time t is calculated using equations (1) and (2), and an absolute value ($I = (Ix^2 + Iy^2)^{1/2}$) of the CAM is computed. Next, the first procedure for the depolarization period ($t_0, t_1, t_2, \ldots, t_m$) is carried out. In the first procedure, a summation of the absolute values of the current arrows is performed until time t_m. Here, the maximum value at time t_m is defined as V_m, and the gap resistance is defined as 1 (uniform value). Next, the second procedure for the repolarization period ($t_m, t_{m+1}, t_{m+2}, \ldots, t_n$) is carried out, and the absolute value is subtracted from V_m until time t_n. Finally, the waveform $V(t)$ can be displayed.

2.3. *Measurement of magnetocardiogram and monophasic action potential*

MCG signals in one patient (female, 37 years old) with type-I LQTS were measured for 30 min by using a SQUID (superconducting quantum interference device) system (MC-6400, Hitachi, Ltd.) with a 64-coaxial gradiometer (Tsukada *et al* 1998, Kandori *et al* 2001a, 2001b). This SQUID was installed in a magnetically shielded room (MSR) with a double mumetal layer. Before the MCG measurement, 12-lead ECG waveforms were obtained for the LQTS patient (figure 5).

Calculation of $Ixy(t)=(Ix(t)^2+Iy(t)^2)^{1/2}$, using a current arrow $(Ix(t), Iy(t))$ at time t

Procedure 1

Depolarization time: $t_0, t_1, t_2, \ldots, t_m$

$$V(t_0) = Ixy(t_0)$$
$$V(t_1) = Ixy(t_0) + Ixy(t_1)$$
$$V(t_2) = Ixy(t_0) + Ixy(t_1) + Ixy(t_2)$$
$$\vdots$$
$$V(t_m) = Ixy(t_0) + Ixy(t_1) + Ixy(t_2) + \ldots + Ixy(t_m) = Vm$$

Procedure 2

Repolarization time: $t_{m+1}, t_{m+2}, t_{m+3}, \ldots, t_n$

$$V(t_{m+1}) = Vm - Ixy(t_{m+1})$$
$$V(t_{m+2}) = Vm - Ixy(t_{m+1}) - Ixy(t_{m+2})$$
$$V(t_{m+3}) = Vm - Ixy(t_{m+1}) - Ixy(t_{m+2}) - Ixy(t_{m+3})$$
$$\vdots$$
$$V(t_n) = Vm - Ixy(t_{m+1}) - Ixy(t_{m+2}) - Ixy(t_{m+3}) - \ldots - Ixy(t_n)$$

Display of V(t) waveform each channel

Figure 4. Flow chart for reconstructing an action potential.

Figure 6 shows the measurement plane in a subject's chest. The sensor array is an 8×8 matrix on a flat plane with a pitch of 25 mm. Each sensor incorporates a first-order gradiometer that has an 18 mm diameter bobbin with a 50 mm long baseline. MCG waveforms of one patient with LQTS were averaged 30 times using the R-wave peak as a trigger.

Standard 6F MAP catheters (EP Technologies Inc.) were used to measure the MAP in the same LQT patient. They were introduced through a femoral vein or an antecubital vein and advanced into the right ventricle and right atrium under fluoroscopic guidance. The MAPs and electrocardiograms from six surface leads were recorded simultaneously from two sites at the right ventricle (RV) by using a contact electrode. The MAP signals were amplified and filtered at a frequency of 0.05–500 Hz. The MAPs were obtained after the placement of the catheter electrode for at least 10 min during both sinus rhythm and constant atrial pacing (cycle length: 500 ms).

The corrected QT interval (QTc) was calculated from Bazett's formula ($QTc = QT/\sqrt{(RR \text{ interval or pacing cycle length})}$). Then QTc was used to adjust the QT intervals between the MAP and the MCG signals.

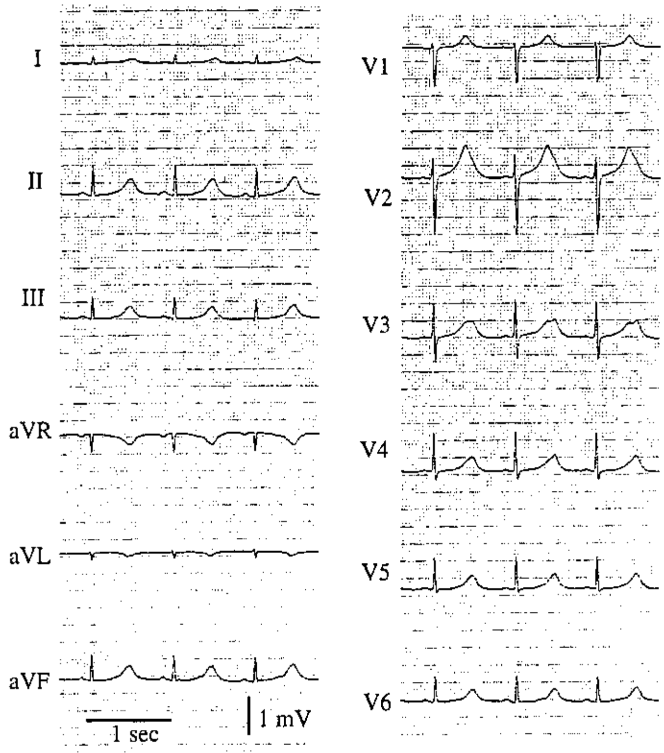

Figure 5. A 12-lead ECG of a patient with type-I LQTS.

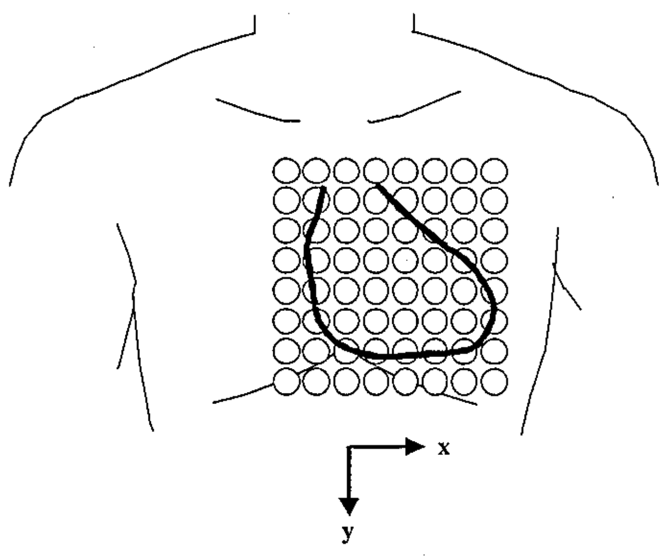

Figure 6. MCG measurement area on the chest of a patient with type-I LQTS.

3. Results

3.1. MCG waveforms and CAMs

The averaged MCG signals of the LQTS patient are shown in figure 7. The QT interval is 678 ms and the QTc interval is 646 ms. The waveform of the signals (in the extended figure)

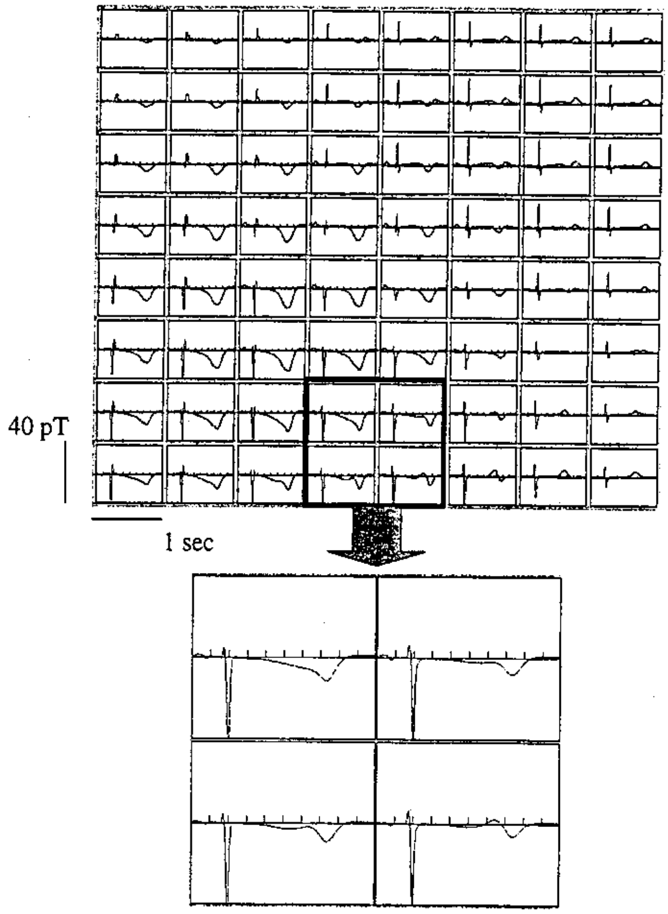

Figure 7. MCG waveforms of a patient with type-I LQTS. Centre lower channels have a notch waveform.

has a notch-type T-wave in the lower right ventricular measurement sites. The 64 waveforms in figure 7 are overlapped on one trace as shown in the upper figure of figure 8. The T-wave shape of the overlapped waveforms has two phases.

Current arrows in the T-wave are derived from the magnetic field of 64 channels at one time using equations (1) and (2). In the top figure, five lines indicate the time at which the CAMs of the lower figure are produced. In the lower figure, an abnormal current arrow with a direction from left to right ventricle (about 135° on the electrical axes) appears during times 1–4. Note that a normal subject shows a similar pattern to line 5 all the time, in which current flows only in one direction (Kandori *et al* 2002). In this case, two different currents were observed, i.e. one directed to the left and the other directed to the right.

3.2. Reconstructed action potential and MAP

The action potential at each channel can be calculated as shown in figure 9 by using the current arrows of figure 8 and the method in figure 4. A strong action potential appears in the lower centre position of the measurement plane. In the case of strong potentials, the action-potential waveform on the right ventricle is shown in the extended lower figure, in which a large and a small notch can be seen.

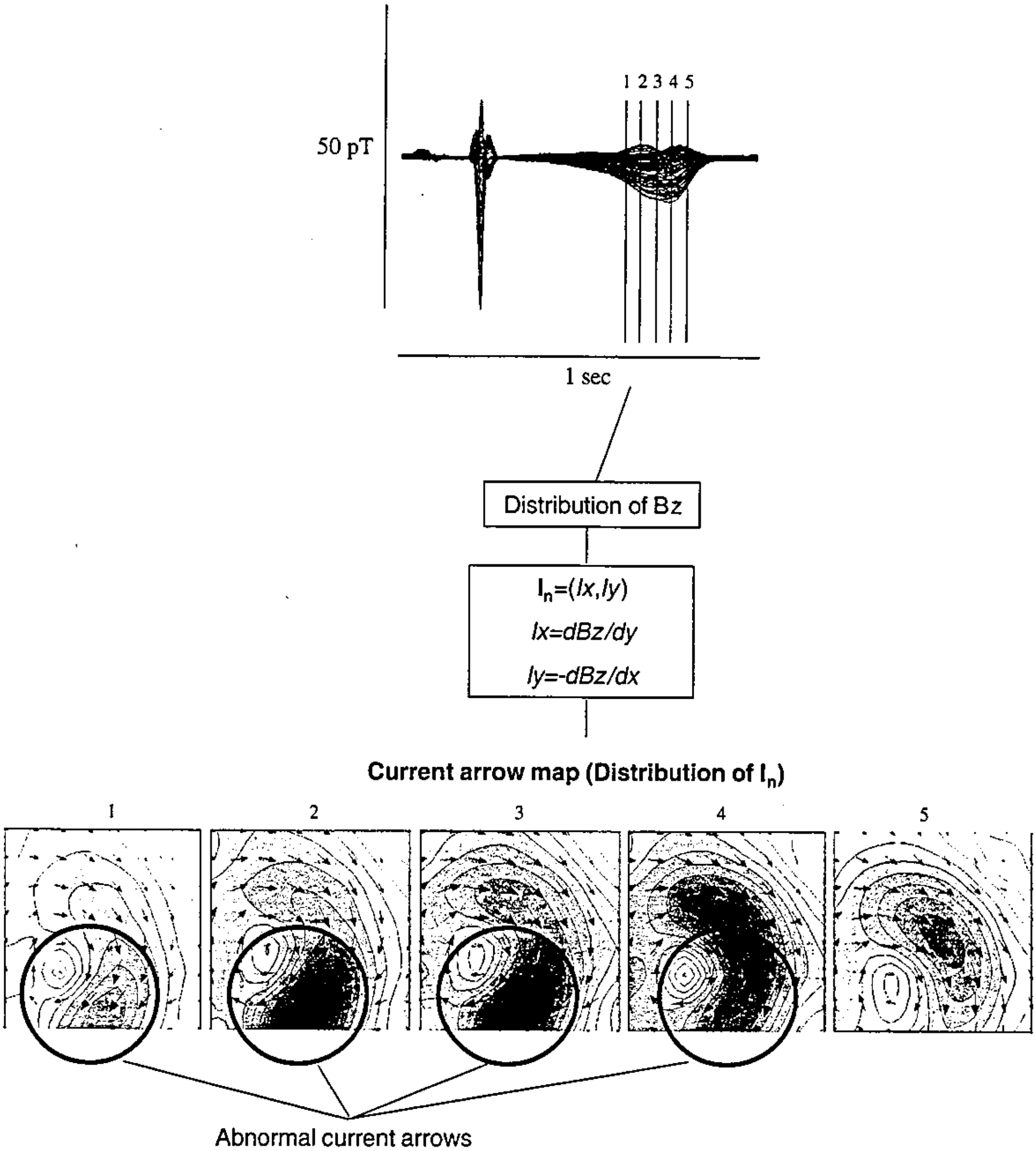

Figure 8. Overlapped MCG waveforms and CAM in a patient with type-I LQTS.

Figure 10(a) shows a recorded MAP waveform in the right ventricle under the pacing condition (500 ms interval). In a simultaneous ECG recording (no figure shown), QTc was 620 ms at V_3. Figure 10(b) indicates the overlapped figure of the MCG waveforms and (c) shows the reconstructed action potential. To compare time variations, the time intervals in these figures are adjusted by using a corrected time (using Bazett's formula). In figure 10(a), early afterdepolarization with a notch shape can be seen. The EAD timing appears in the second phase on the MCG waveforms and in the small notch on the reconstructed action-potential waveform.

Comparing the reconstructed waveforms and CAM in figure 8 shows that the abnormal current arrows appear to move from the large notch to the small notch. On the other hand, the EAD in the MAP can be seen at the time of the small notch.

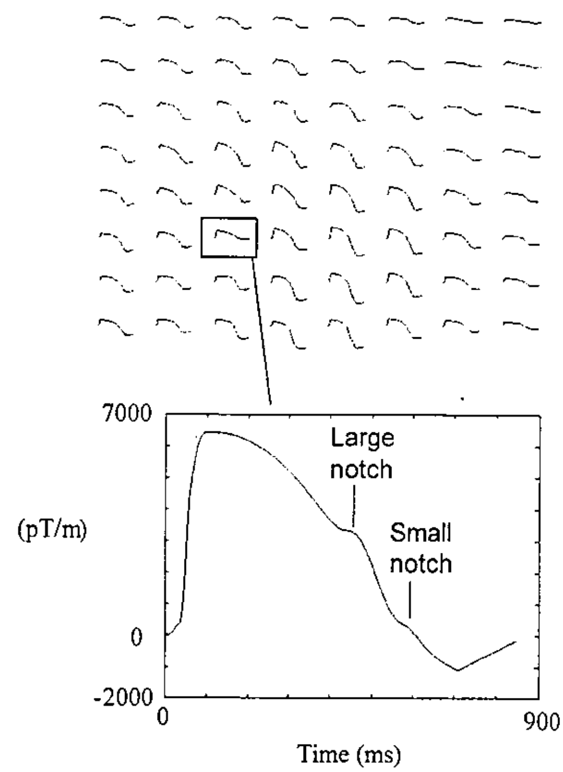

Figure 9. Reconstructed action-potential waveforms. Large and small notches appear on the right ventricular side.

4. Discussion

Our reconstructed action potential has a totally different basis from the MAP recording, which is a good indicator of the action-potential duration. The MCG measures magnetic flux density as a result of tangential current density where the majority of currents are wiping out one another. A reconstruction of the action potential from these data is limited, because different types of electrically active cardiomyocytes differ in action-potential duration, e.g. M-cells which play a special role in action-potential duration and long-QT syndrome (Antzelevitch and Shimizu 2002). In short, measurements of magnetic fields outside the body characterize the sum vector of these forces, but the reconstructed action potential does not differentiate between the underlying contributions of the different cell categories. Therefore, the reconstruction method can be used, provided that we understand the difference.

In this study, we used a simple calculation (summation and subtraction) of the current arrows during the repolarization period (QRS complex and ST-T wave). Interestingly, the calculated waveform (second small notch) is similar to the MAP pattern in the late T-wave. It was found that the appearance timing agrees with the EAD occurrence, because there is a similarity between the QTc of 646 ms in the MCG and 620 ms in the MAP. This similarity (second small notch) could indicate the applicability of the calculation. However, the reconstructed pattern only has a large notch in the early T-wave. The difference between the MAP and the reconstructed data might be caused by different sites and times in the measurement of the right ventricular muscle. Furthermore, MCG data have a tendency to reflect the potential on the epicardial muscle surface of the heart, and MAP data reflect the potential on the endocardial muscle surface of the heart. Although there are physical

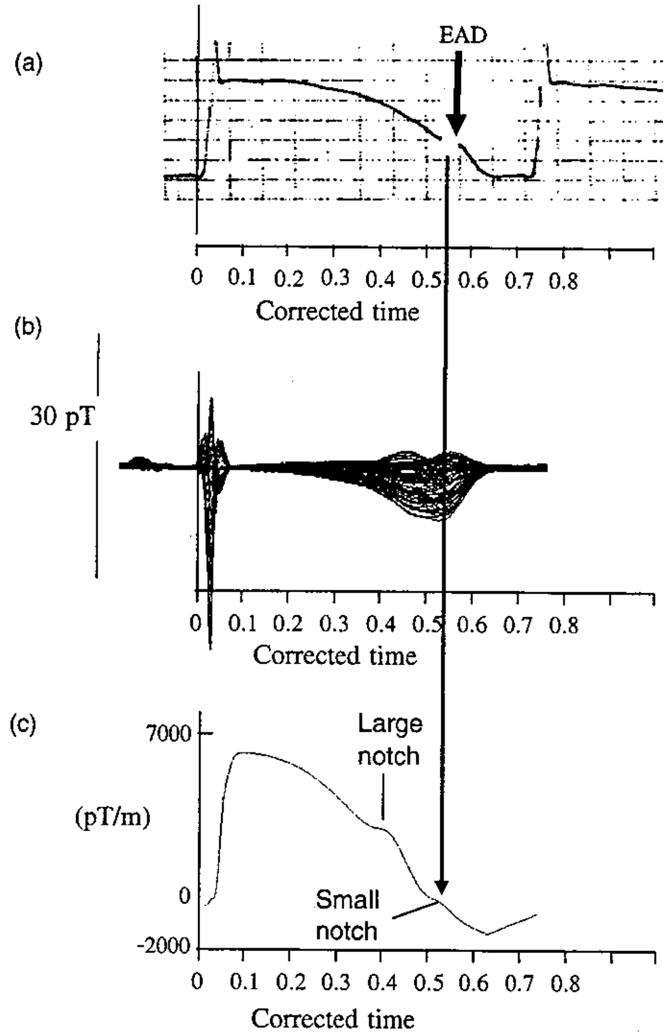

Figure 10. Comparison between reconstructed action-potential waveforms and a MAP waveform. Occurrence timing of the small notch coincides with EAD timing. MCG data in figures 10(b) and (c) show one beat signal.

differences as mentioned above, the reconstructed action potential could help us to understand the cell-membrane electrical activation.

Although there are differences between the MCG and the MAP, it is very interesting that the initiation time of an abnormal current distribution coincides with the first large notch, and its end time coincides with the second small notch, which may be associated with EAD in the MAP. Because the EAD triggered the ventricular premature complex (Shimizu *et al* 1994) or *torsades de pointes* in long-QT-syndrome patients (Kurita *et al* 1997), the abnormal current might cause a spatial dispersion at the ending point. Furthermore, the abnormality may be a dangerous sign of ventricular tachycardia, etc.

On the other hand, it is very difficult to reconstruct the action potential by using ECG signals, because an electrical distribution in the heart cannot be calculated. Furthermore the ECG signals have a distortion due to a different conductivity such as the lungs and the bones.

In conclusion, the calculation method presented in this study demonstrated the possibility of reconstructing an action potential in the depolarization period by using non-invasive MCG data. Furthermore, an analysis using both the reconstructed action potential and the CAM provided new clinical information such as EAD appearance and the ventricular premature complex. The simple reconstruction method described here can thus elicit the mechanism of electrical activation in the myocardial muscle in patients with an abnormal repolarization.

4.1. Study limitation

There are several limitations in the present study. First, we need a lot of MCG signals in LQT patients with EAD appearing in a catheter MAP, and the reconstructed action potential of normal cases must be compared with MAP. Second, a current arrow has a limitation that it does not express the real physical current on the ventricular muscle.

Acknowledgments

We thank Ito Sonoe, Syuji Hashimoto, Norio Tanaka and Kiichi Masuda of the National Cardiovascular Center for doing the MCG measurements.

References

Antzelevitch C and Shimizu W 2002 Cellular mechanisms underlying the long QT syndrome *Curr. Opin. Cardiol.* **17** 43–51

Beeler G W and Reuter H 1977 Reconstruction of the action potential of ventricular myocardial fibres *J. Physiol.* **268** 177–210

Bonatti V, Rolli A and Botti G 1983 Recordings of monophasic action potentials of the right ventricle in long QT syndromes complicated by severe ventricular arrhythmias *Eur. Heart J.* **4** 168–79

Cuffin B N 1978 Of the use of electric and magnetic data to determine electric sources in a volume conductor *Ann. Biomed. Eng.* **6** 173–93

Delgado C, Steinhaus B, Delmar M, Chialvo D R and Jalife J 1990 Directional differences in excitability and margin of safety for propagation in sheep ventricular epicardial muscle *Circ. Res.* **67** 97–110

Gavrilescu S and Luca C 1978 Right ventricular monophasic action potentials in patients with long QT syndrome *Br. Heart J.* **40** 1014–8

Hoffman B F and Cranefield P F 1960 *Electrophysiology of the Heart* (New York: McGraw-Hill)

Hoffman B F, Cranefield P F, Lepeschkin E, Surawicz B and Herrlich H C 1959 Comparison of cardiac monophasic action potentials recorded by intracellular and suction electrodes *Am. J. Physiol.* **196** 1297–301

Horigome H, Tsukada K, Kandori A, Shiono J, Matsui A, Terada Y and Mitsui T 1999 Visualization of regional myocardial depolarization by tangential component mapping on magnetocardiogram in children *Int. J. Cardiac. Imaging* **15** 331–7

Hosaka H and Cohen D 1976 Visual determination of generators of the magnetocardiogram *J. Electrocardiol.* **9** 426–32

Kandori A, Kanzaki H, Miyatake K, Hashimoto S, Itoh S, Tanaka N, Miyashita T and Tsukada K 2001a A method for detecting myocardial abnormality by using a total current-vector calculated from ST-segment deviation of a magnetocardiogram signal *Med. Biol. Eng. Comput.* **39** 21–8

Kandori A, Kanzaki H, Miyatake K, Hashimoto S, Itoh S, Tanaka N, Miyashita T and Tsukada K 2001b A method for detecting myocardial abnormality by using a current-ratio map calculated from an exercise-induced magnetocardiogram *Med. Biol. Eng. Comput.* **39** 29–34

Kandori A *et al* 2002 Detection of spatial repolarization abnormalities in patients with LQT1 and LQT2 forms of congenital long-QT syndrome *Physiol. Meas.* **23** 603–14

Kanzaki H, Nakatani S, Kandori A, Tsukada K and Miyatake K 2003 A new screening method to diagnose coronary artery disease using multichannel magnetocardiogram and simple exercise *Basic Res. Cardiol.* **98** 124–32

Karp P J, Katila T E and Saarinen M 1980 The normal human magnetocardiogram: II. A multiple analysis *Circ. Res.* **47** 117–30

Kurita T, Ohe T, Shimizu W, Suyama K, Aihara N, Takaki H, Kamakura S and Shimomura S 1997 Early afterdepolarization like activity in patients with class IA induced long QT syndrome and Torsades de Pointes *PACE* **20** 695–705

Miyashita T, Kandori A and Tsukada K 1998 Construction of tangential vectors from normal cardiac magnetic field components *Proc. 20th Int. Conf. IEEE/EMBS (Hong Kong)* pp 520–3

Nenonen J, Purcell C J, Horacek B M, Stroink G and Katila T 1991 Magnetocardiographic functional localization using a current dipole in a realistic torso *IEEE Trans. Biomed. Eng.* **38** 658–64

Roberge F A, Vinet A and Victorri B 1986 Reconstruction of propagated electrical activity with a two-dimensional model of anisotropic heart muscle *Circ. Res.* **58** 461–75

Shimizu W, Ohe T, Kurita T, Kawade M, Arakaki Y, Aihara N, Kamakura S, Kamiya T and Shimomura K 1995 Effects of verapamil and propranolol on early afterdepolarization and ventricular arrhythmias induced by epinephrine in congential long QT syndrome *J. Am. Coll. Cardiol.* **26** 1299–309

Shimizu W, Ohe T, Kurita T, Takaki H, Aihara N, Kamakura S, Matsuhisa M and Shimomura K 1991 Early afterdepolarizations induced by isoproterenol in patients with congenital long QT syndrome *Circulation* **84** 1915–23

Shimizu W, Ohe T, Kurita T, Tokuda T and Shimomura K 1994 Epinephrine-induced ventricular premature complexes due to early afterdepolarizations and effects of verapamil and propranolol in a patient with congenital long QT syndrome *J. Cardiovasc. Electrophysiol.* **5** 438–44

Tsukada K, Kandori A, Miyashita T, Sasabuti H, Suzuki H, Kondo S, Komiyama Y and Teshigawara K 1998 A simplified superconducting interference device system to analyze vector components of a cardiac magnetic field *Proc. 20th Int. Conf. IEEE/EMBS (Hong Kong)* pp 524–7

Tsukada K, Mitsui T, Terada Y, Horigome H and Yamaguchi I 1999 Non invasive visualization of multiple simultaneously activated regions on torso magnetocardiographic maps during ventricular depolarization *J. Electrocardiol.* **32** 305–13

Vos M A, Gorenek B, Verduyn S C, van der Hulst F F, Leunissen J D, Dohmen L and Wellens H J 2000 Observations on the onset of Torsade de Pointes arrhythmias in the acquired long QT syndrome *Cardiovasc. Res.* **48** 421–9

Diagnostic value of epinephrine test for genotyping LQT1, LQT2, and LQT3 forms of congenital long QT syndrome

Wataru Shimizu, MD, PhD,[a,b] Takashi Noda, MD, PhD,[a] Hiroshi Takaki, MD,[c] Noritoshi Nagaya, MD, PhD,[a] Kazuhiro Satomi, MD,[a] Takashi Kurita, MD, PhD,[a] Kazuhiro Suyama, MD, PhD,[a] Naohiko Aihara, MD,[a] Kenji Sunagawa, MD, PhD,[c] Shigeyuki Echigo, MD,[d] Yoshihiro Miyamoto, MD, PhD,[b] Yasunao Yoshimasa, MD, PhD,[b] Kazufumi Nakamura, MD, PhD,[e] Tohru Ohe, MD, PhD,[e] Jeffrey A. Towbin, MD,[f] Silvia G. Priori, MD, PhD,[g] Shiro Kamakura, MD, PhD[a]

[a]From the Division of Cardiology, Department of Internal Medicine, National Cardiovascular Center, Suita, Japan,
[b]Laboratory of Molecular Genetics, National Cardiovascular Center, Suita, Japan,
[c]Department of Cardiovascular Dynamics, National Cardiovascular Center, Suita, Japan,
[d]Department of Pediatrics, National Cardiovascular Center, Suita, Japan,
[e]Department of Cardiovascular Medicine, Okayama University Graduate School of Medicine and Dentistry, Okayama, Japan,
[f]Department of Pediatrics (Cardiology), Molecular & Human Genetics, Baylor College of Medicine, Houston, Texas, and
[g]Molecular Cardiology, Salvatore Maugeri Foundation, IRCCS, Pavia, Italy.

OBJECTIVES The aim of this study was to test the hypothesis that epinephrine test may have diagnostic value for genotyping LQT1, LQT2, and LQT3 forms of congenital long QT syndrome (LQTS).

BACKGROUND A differential response of dynamic QT interval to epinephrine infusion between LQT1, LQT2, and LQT3 syndromes has been reported, indicating the potential diagnostic value of the epinephrine test for genotyping the three forms.

METHODS The responses of 12-lead ECG parameters to epinephrine were retrospectively examined in 15 LQT1, 10 LQT2, 8 LQT3, and 10 healthy volunteers to select the best ECG criteria for separating the four groups. The epinephrine test then was prospectively conducted in 42 probands clinically affected with LQTS, their 67 family members, and 10 new volunteers. The best criteria were applied in a blinded fashion to prospectively separate a different group of 31 LQT1, 23 LQT2, 6 LQT3, and 30 Control patients (10 genotype-negative LQT1, 10 genotype-negative LQT2 family members, and 10 volunteers).

RESULTS The sensitivity (penetrance) by ECG diagnostic criteria was lower in LQT1 (68%) than in LQT2 (83%) or LQT3 (83%) before epinephrine and was improved with steady-state epinephrine in LQT1 (87%) and LQT2 (91%) but not in LQT3 (83%), without the expense of specificity (100%). The sensitivity and specificity to differentiate LQT1 from LQT2 were 97% and 96%, those from LQT3 were 97% and 100%, and those from Control were 97% and 100%, respectively, when Δ mean corrected Q-Tend $\geq$35ms at steady state was used. The sensitivity and specificity to differentiate LQT2 from LQT3 or Control were 100% and 100%, respectively, when Δ mean corrected Q-Tend $\geq$80ms at peak was used.

CONCLUSIONS Epinephrine infusion is a powerful test to predict the genotype of LQT1, LQT2, and LQT3 syndromes as well as to improve the clinical diagnosis of genotype-positive patients, especially those with LQT1 syndrome.

KEYWORDS Arrhythmia; Diagnosis; Long QT syndrome; Catecholamines; Genes

1547-5271/$ -see front matter © 2004 Heart Rhythm Society. All rights reserved.
doi:10.1016/j.hrthm.2004.04.021

Table 1 Clinical characteristics of LQT1, LQT2, LQT3, and control groups in prospective study

	LQT1 (n = 31)	LQT2 (n = 23)	LQT3 (n = 6)	Control (n = 30)
Age [yr (range)]	21 ± 14 (4–55)	27 ± 16 (6–61)	21 ± 16 (7–43)	29 ± 15 (6–64)
Age <15 yr	16/31 (52%)	7/23 (30%)	3/6 (50%)	5/30 (17%)
Female sex	17/31 (55%)	16/23 (70%)	3/6 (50%)	16/30 (53%)
Baseline heart rate (beats/min)	67 ± 9	66 ± 12	60 ± 10	72 ± 13
Peak heart rate with Epi (beats/min)	99 ± 14	96 ± 16	95 ± 10	99 ± 13
Steady-state heart rate with Epi (beats/min)	85 ± 12	76 ± 14	70 ± 12	79 ± 13
Baseline QTc interval (ms)	470 ± 41†	503 ± 33*	506 ± 41*	408 ± 19
Syncope or aborted cardiac arrest	14/31 (45%)	12/23 (52%)	2/6 (33%)	(0%)
Beta-blockers	(0%)	(0%)	(0%)	(0%)

Values are given as mean ± SD where indicated. Epi = epinephrine; QTc = corrected QT.
*P < 0.05 vs LQT1 and control.
†P < 0.05 vs control.

The congenital long QT syndrome (LQTS) is a hereditary disorder caused by mutations in genes of the potassium and sodium channels or membrane adapter located on chromosomes 3, 4, 7, 11, 17, and 21.[1–4] Among the LQT1, LQT2, and LQT3 forms, which account for approximately two thirds of genotyped patients, cardiac events are more often associated with sympathetic stimulation (physical or emotional stress) in LQT1 than in either LQT2 or LQT3 syndrome.[5–8] Concordant with the influence of sympathetic stimulation, beta-blockers are the most effective in LQT1 syndrome.[9,10] Therefore, genotyping of LQTS is of major importance because it would be helpful in managing and treating patients more effectively.[11] Preliminary studies by our and other groups have demonstrated the differential response of dynamic QT interval to epinephrine infusion between LQT1, LQT2, and LQT3 syndromes,[12,13] indicating the potential diagnostic value of the epinephrine test for genotyping the three forms. The present study was designed to test this hypothesis.

Methods

Study design and population

First, we retrospectively analyzed the response of ECG parameters to epinephrine infusion in 15 LQT1 patients (5 families), 10 LQT2 patients (5 families), 8 LQT3 patients (2 families), and 10 healthy volunteers (Control), some of whom were included in our previous study.[12] The best ECG criteria separating LQT1, LQT2, LQT3, and Control patients were selected. Then, we prospectively conducted an epinephrine test in 42 probands who were clinically diagnosed as having congenital LQTS, their 67 family members, and 10 new healthy volunteers. The best ECG criteria with the epinephrine test derived from the retrospective study were applied in a blinded fashion to differentiate LQT1, LQT2, LQT3, and Control groups in a total of 119 subjects. Molecular screening, which was performed after the epinephrine test, identified 31 genotype-positive LQT1 patients (12 families), 23 genotype-positive LQT2 patients (12 families), 6 genotype-positive LQT3 patients (3 families), 10 genotype-negative LQT1 patients (9 families), and 10 genotype-negative LQT2 patients (4 families). The study population of the prospective study included the 31 LQT1, 23 LQT2, and 6 LQT3 patients. The data from the 10 genotype-negative LQT1 patients, 10 genotype-negative LQT2 patients, and 10 healthy volunteers were pooled and referred to as Control group, because there were no significant differences in the clinical and ECG characteristics among the three groups. In the remaining 29 patients including 15 probands (15 families), no responsible mutations were identified in any LQTS genes. There were no significant differences among LQT1, LQT2, LQT3, and Control groups with regard to age, percentage of age <15 years old, gender, baseline heart rate, and peak and steady-state heart rate with epinephrine in the prospective study (Table 1). Percentage of syncope or aborted cardiac arrest was no different among LQT1, LQT2, and LQT3 groups (Table 1). The baseline corrected QT intervals in LQT2 and LQT3 groups were significantly longer than that in the LQT1 group; those in the LQT1, LQT2, and LQT3 groups were all significantly longer than that in the Control group (Table 1). Genotyping of LQTS was reviewed and approved by our Ethical Review Committee, and written informed consent was obtained from all patients or their parents when the patients were younger than 20 years. All epinephrine tests were conducted in the National Cardiovascular Center as part of a clinical

Dr. Shimizu was supported in part by the Japanese Cardiovascular Research Foundation, Vehicle Racing Commemorative Foundation, and Health Sciences Research Grants from the Ministry of Health, Labour and Welfare, and Research Grant for Cardiovascular Diseases (15C-6) from the Ministry of Health, Labour and Welfare, Japan. Dr. Priori was supported by an educational grant from the Leducq Foundation. Dr. Towbin was supported by grants from the National Institutes of Health (NIH), National Heart, Lung & Blood Institute (NHLBI) (R01 HL33843 and R01 HL51618).

Address reprint requests and correspondence: Dr. Wataru Shimizu, Division of Cardiology, Department of Internal Medicine, National Cardiovascular Center, 5-7-1 Fujishiro-dai, Suita, Osaka, 565-8565 Japan.
E-mail address: wshimizu@hsp.ncvc.go.jp.

(Received January 30, 2004; accepted April 14, 2004.)

evaluation of LQTS patients. We previously reported that the oral beta-blocker propranolol (0.5–2 mg/kg) completely suppressed the effects of epinephrine on repolarization parameters[14]; therefore, no subjects took beta-blockers at the time of the epinephrine test in either the retrospective or prospective study. Among a total of 93 genotyped LQTS patients in the retrospective and prospective studies, 85 patients were transferred to our hospital for initial evaluation of LQTS without any medications including beta-blockers, and the epinephrine test could be conducted in the absence of beta-blockers. Appropriate therapies, including beta-blockers, were started after the evaluation of LQTS. In the remaining 8 patients (3 LQT1 and 5 LQT2), beta-blockers were withheld during the evaluation of LQTS, including the epinephrine test, and then reinstated.

Clinical diagnosis

LQTS-affected individuals were diagnosed based on the ECG criteria of Keating et al,[15] including a corrected QT ≥470 ms in asymptomatic individuals and a corrected QT >440 ms for males and >460 ms for females associated with ≥1 of the following: (1) stress-related syncope, (2) documented torsades de pointes, or (3) family history of early sudden cardiac death. The LQTS score was calculated using the diagnostic criteria of Schwartz et al.[16]

Recording of standard 12-lead ECG

A standard 12-lead ECG was recorded using an FDX6521 (Fukuda Denshi Co., Tokyo, Japan) with the patient in the supine position. These ECG data were digitized using analog-to-digital converters at a sampling rate of 1,000 samples per second per channel.

Measurements

Measurement of the ECG parameters was performed against five averaged QRS complexes by an off-line computer with an analysis program developed by our institution. Q-Tend was defined as the interval between QRS onset and the point at which an isoelectric line intersected a tangential line drawn at the minimum dV/dt point of a positive T wave or at the maximum dV/dt point of a negative T wave. When a bifurcated or secondary T wave (pathologic U wave) appeared, it was included as part of the measurement of the Q-Tend, but a normal U wave, which was apparently separated from a T wave, was not included. Q-Tpeak was defined as the interval between QRS onset and the peak of the positive T wave or the nadir of the negative T wave. When the T wave had a biphasic or a notched configuration, the peak of the T wave was defined as that of dominant T deflection. Q-Tend, Q-Tpeak, and Tpeak-end (Q-Tend − Q-Tpeak) as an index of transmural dispersion of repolarization were measured automatically from all 12-lead ECGs, corrected by Bazett's method, and averaged among all 12 leads. Data of corrected Q-Tend, Q-Tpeak, and Tpeak-end, which were measured simply from lead V_5, also were evaluated. As an index of spatial dispersion of repolarization, dispersion of the corrected Q-Tend was defined as the interval between the maximum and the minimum of the corrected Q-Tend among the 12 leads.

Epinephrine administration

A bolus injection of epinephrine (0.1 μg/kg) was immediately followed by continuous infusion (0.1 μg/kg/min). The 12-lead ECG was continuously recorded during sinus rhythm under baseline conditions and usually for 5 minutes under epinephrine infusion. The effect of epinephrine on both RR and QT intervals usually reached steady-state conditions 2 to 3 minutes after the start of epinephrine infusion. Epinephrine infusion for >5 minutes was avoided, and ECG monitoring was continued for another 5 minutes after epinephrine infusion to detect the possible occurrence of torsades de pointes. The ECG data as a representative of the peak epinephrine effect were collected 1 to 2 minutes after the start of epinephrine infusion when the RR interval was the shortest, whereas the data as a representative of the steady-state epinephrine effect were collected 3 to 5 minutes after the start of epinephrine infusion.

Statistical analysis

Data are expressed as mean ± SD, except for those shown in Figure 3, which are expressed as mean ± SEM. Repeated-measures two-way ANOVA followed by the Scheffé test was used to compare measurements made before and after epinephrine infusion and to compare differences between groups (STATISTICA, 98 Edition). Repeated-measures one-way ANOVA followed by the Scheffé test was used to compare changes (Δ) in the measurements with epinephrine between groups. Differences in frequencies were analyzed by Chi-square test. A two-sided $P < .05$ was considered statistically significant.

Results

Retrospective study

Best ECG criteria to differentiate LQT1, LQT2, LQT3, and Control groups

The retrospective study as well as our previous study[12] suggested the differential response of the mean corrected Q-Tend interval to epinephrine test among LQT1, LQT2, and LQT3 groups. The mean corrected Q-Tend intervals were more prominently prolonged at peak epinephrine effect in LQT1 and LQT2 groups than in either the LQT3 or the Control group. On the other hand, they remained pro-

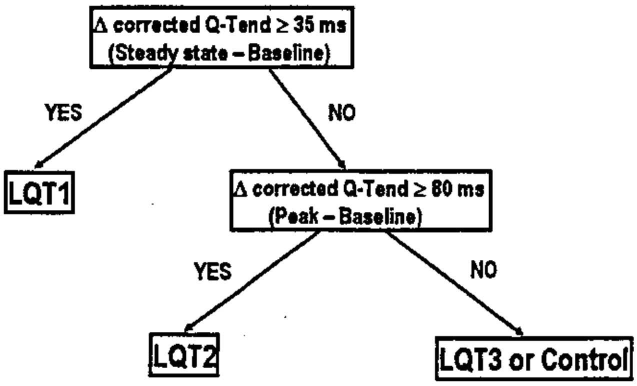

Figure 1 Flow chart for predicting genotype with the epinephrine test.

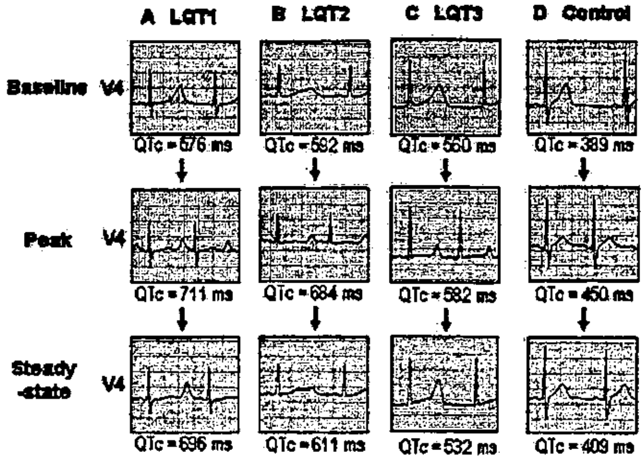

Figure 2 ECG lead V_4 under baseline conditions and at peak and steady-state epinephrine effects in LQT1 **(A)**, LQT2 **(B)**, LQT3 **(C)**, and Control **(D)** patients. The mean corrected Q-Tend was prominently prolonged from 576 to 711 ms at peak epinephrine effect and remained prolonged at steady state (696 ms) in the LQT1 patient. In the LQT2 patient, the mean corrected Q-Tend also was dramatically prolonged from 592 to 684 ms at peak but returned to the baseline level at steady-state (611 ms). It was much less prolonged (LQT3: 560 to 582 ms, Control: 389 to 450 ms) at peak in the LQT3 and Control patients than in either the LQT1 or LQT2 patient and was shortened to the baseline level at steady state (532, 409 ms).

longed at steady-state epinephrine effect only in the LQT1 group but not in the other three groups.

Figure 1 illustrates a flow chart for predicting LQT1, LQT2, LQT3, and Control patients with the epinephrine test derived from the retrospective study. If the Δ mean corrected Q-Tend was ≥35 ms at steady-state epinephrine effect, the patient was expected to be affected with LQT1 syndrome. If not, and the Δ mean corrected Q-Tend was ≥80 ms at peak epinephrine effect, the patient was expected to be linked to LQT2 syndrome. If not, the patient was expected to be an LQT3 or Control patient.

Prospective study

Differential responses of ECG parameters to epinephrine infusion

Figure 2 illustrates ECG lead V_4 under baseline conditions and at peak and steady-state epinephrine effects in representative LQT1, LQT2, LQT3, and Control patients.

Figure 3 shows composite data of the ECG parameters under baseline conditions and at peak and steady-state epinephrine effects in the four groups of the prospective study. Under baseline conditions, the mean corrected Q-Tend and Q-Tpeak were significantly longer in the LQT1, LQT2, and LQT3 groups than in the Control group; both were significantly longer in the LQT2 and LQT3 groups than in LQT1 group (Figure 3A and 3B). The mean corrected Tpeak-end was significantly greater in the LQT2 group than in the LQT3 or Control group (Figure 3C). The dispersion of corrected Q-Tend was significantly larger in the LQT1 and LQT2 groups than in the Control group (Figure 3D). The mean corrected Q-Tend and Q-Tpeak were dramatically prolonged at peak epinephrine effect (470 ± 41 to 596 ± 56 ms, 385 ± 34 to 480 ± 53 ms; $P < .05$, respectively) and remained prolonged at steady state (549 ± 55 ms, 438 ± 50 ms; $P < .05$ vs baseline, respectively) in the LQT1 group (Figure 3A and 3B, closed circles). The mean corrected Tpeak-end also was markedly increased at peak epinephrine effect (85 ± 11 to 115 ± 19 ms; $P < .05$), and remained increased at steady state (111 ± 17 ms; $P < .05$ vs baseline) as a result of a greater prolongation in the mean corrected Q-Tend than in the mean corrected Q-Tpeak at both peak and steady-state conditions (Figure 3C, closed circles). The mean corrected Q-Tend and Q-Tpeak also were dramati-

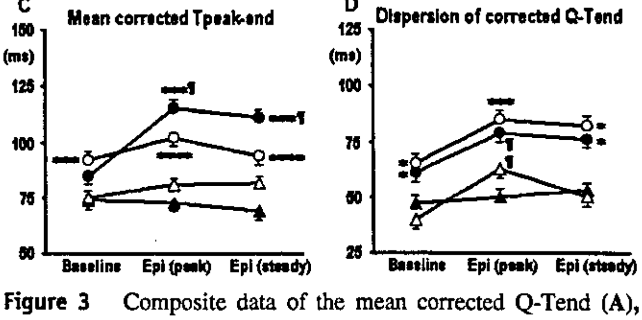

Figure 3 Composite data of the mean corrected Q-Tend **(A)**, Q-Tpeak **(B)**, Tpeak-end **(C)**, and dispersion of corrected Q-Tend **(D)** under baseline conditions and at peak and steady-state epinephrine effects in LQT1 *(closed circle)*, LQT2 *(open circle)*, LQT3 *(closed triangle)*, and Control *(open triangle)* groups of the prospective study. *$P < .05$ vs Control; **$P < .05$ vs LQT1 and Control; ***$P < .05$ vs LQT3 and Control; ****$P < .05$ vs LQT1, LQT3, and Control; ¶$P < .05$ vs baseline.

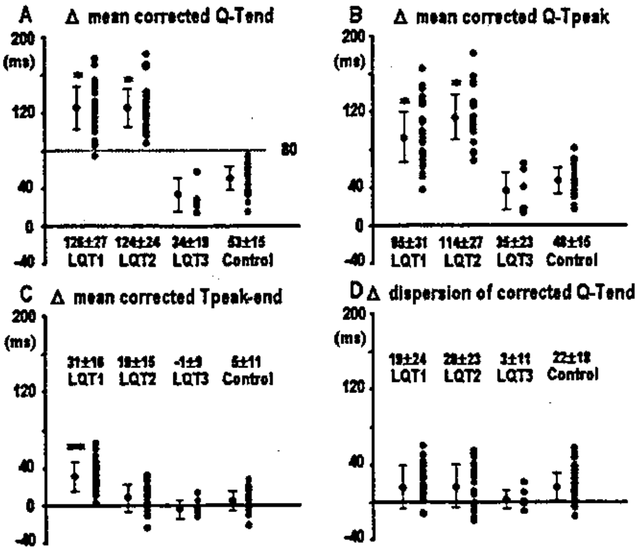

Figure 4 Composite data of changes (Δ) in the mean corrected Q-Tend (A), Q-Tpeak (B), Tpeak-end (C), and dispersion of corrected Q-Tend (D) between baseline conditions and peak epinephrine effects in LQT1, LQT2, LQT3, and Control groups of the prospective study. *$P < .05$ vs LQT3 and Control; **$P < .05$ vs LQT2, LQT3 and Control.

cally prolonged at peak epinephrine effect (503 ± 33 to 627 ± 30 ms, 411 ± 26 to 525 ± 32 ms; $P < .05$, respectively) in the LQT2 group but returned to baseline levels at steady state (518 ± 38 ms, 424 ± 36 ms; P = NS vs baseline, respectively; Figure 3A and 3B, open circles). The mean corrected Tpeak-end was unchanged with epinephrine (92 ± 23 to 102 ± 18 to 94 ± 19 ms) in the LQT2 group (Figure 3C, open circles). The mean corrected Q-Tend and Q-Tpeak were much less prolonged at peak epinephrine effect (LQT3: 506 ± 41 to 540 ± 28 ms; P = NS, 432 ± 40 to 467 ± 26 ms; P = NS, Control: 408 ± 19 to 461 ± 19 ms, 332 ± 17 to 380 ± 23 ms; $P < .05$, respectively) in the LQT3 and Control groups than in the LQT1 or LQT2 group and were shortened to the baseline levels at steady state (LQT3: 496 ± 37 ms, 427 ± 30 ms; Control: 415 ± 18 ms, 333 ± 19 ms; P = NS vs baseline, respectively) (Figure 3A and 3B, closed triangles and open triangles). The mean corrected Tpeak-end was unchanged with epinephrine (LQT3: 74 ± 7 to 73 ± 4 to 69 ± 10 ms; Control: 75 ± 8 to 81 ± 13 to 82 ± 11 ms) in the LQT3 and Control groups (Figure 3C, closed triangles and open triangles). The dispersion of corrected Q-Tend was increased at peak epinephrine effect in the LQT1 and Control groups (LQT1: 61 ± 21 ms, 79 ± 27 ms; Control: 40 ± 14 ms, 63 ± 19 ms; $P < .05$, respectively).

Figure 4 illustrates the changes (Δ) in the ECG parameters between baseline conditions and peak epinephrine effects in the four groups of the prospective study. Both the Δ mean corrected Q-Tend and Q-Tpeak were no different between the LQT1 and LQT2 groups, but they were significantly greater than those in the LQT3 and Control groups ($P < .05$; Figure 4A and 4B). No significant differences were observed in the Δ mean corrected Q-Tend and Q-Tpeak between the LQT3 and Control groups. The Δ mean corrected Tpeak-end was significantly greater in the LQT1 group than in the other three groups ($P < .05$; Figure 4C). No significant differences were observed in the Δ dispersion of corrected Q-Tend among the four groups (Figure 4D). As suggested by the retrospective study, the Δ mean corrected Q-Tend ≥80 ms at peak epinephrine effect could most effectively differentiate the LQT1 and LQT2 groups from the LQT3 or Control group (Figure 4A).

Figure 5 illustrates Δ in the ECG parameters between baseline conditions and steady-state epinephrine effects in the four groups of the prospective study. The Δ mean corrected Q-Tend, Q-Tpeak, and Tpeak-end were significantly greater in LQT1 than in the other three groups ($P < .05$; Figure 5A–5C). The Δ mean corrected Q-Tend was significantly larger in the LQT2 than in LQT3 group ($P < .05$; Figure 5A). There were no significant differences in the Δ dispersion of corrected Q-Tend among the four groups (Figure 5D). As suggested by the retrospective study, the Δ mean corrected Q-Tend ≥35 ms at steady-state epinephrine effect could most effectively differentiate the LQT1 group from the other three groups (Figure 5A).

Improvement of clinical diagnosis with epinephrine test

The sensitivity (i.e., penetrance) and specificity for identifying genotype-positive LQT1, LQT2, and LQT3 patients by the ECG diagnostic criteria before and after steady-state epinephrine effects were evaluated in the prospective study.

The sensitivity for identifying genotype-positive LQT1 patients among the LQT1 and Control groups was low under baseline conditions; 68% (21/31) using the ECG

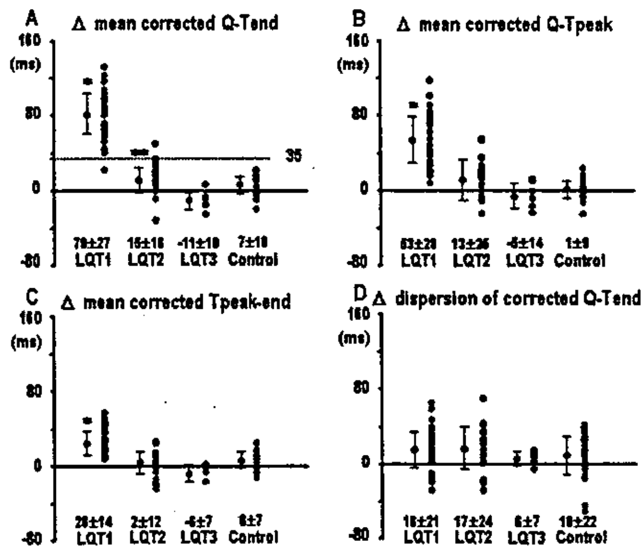

Figure 5 Composite data of changes (Δ) in the mean corrected Q-Tend (A), Q-Tpeak (B), Tpeak-end (C), and dispersion of corrected Q-Tend (D) between baseline conditions and steady-state epinephrine effects in LQT1, LQT2, LQT3 and Control groups of the prospective study. *$P < .05$ vs LQT2, LQT3 and Control; **$P < .05$ vs LQT3.

Table 2 Prediction of genotype with the epinephrine test in prospective study

	Sensitivity	Specificity	Positive predictive value	Negative predictive value	Accuracy
LQT1 vs LQT2	97%	96%	97%	96%	96%
Δ Mean corrected Q-Tend ≥35 ms (Steady state-Baseline)	(90%)	(83%)	(88%)	(86%)	(87%)
LQT1 vs LQT3	97%	100%	100%	86%	97%
Δ Mean corrected Q-Tend ≥35 ms (Steady state-Baseline)	(90%)	(100%)	(100%)	(67%)	(92%)
LQT1 vs control	97%	100%	100%	97%	98%
Δ Mean corrected Q-Tend ≥35 ms (Steady state-Baseline)	(90%)	(97%)	(97%)	(91%)	(93%)
LQT2 vs LQT3	100%	100%	100%	100%	100%
Δ Mean corrected Q-Tend ≥80 ms (Peak-Baseline)	(91%)	(100%)	(100%)	(75%)	(93%)
LQT2 vs control	100%	100%	100%	100%	100%
Δ Mean corrected Q-Tend ≥80 ms (Peak-Baseline)	(91%)	(90%)	(88%)	(93%)	(91%)

Percentages in parentheses indicate those calculated by data measured simply from ECG lead V_5. Δ-Increase with epinephrine.

diagnostic criteria, 68% (21/31) when an LQTS score ≥4 was used, and 74% (23/31) when a score ≥2 was used. The specificity was 100% (30/30) regardless of the criteria. The sensitivity was substantially improved by measurement of the mean corrected Q-Tend at steady-state epinephrine effect without the expense of specificity (100% [30/30]); 87% (27/31), 81% (25/31), and 90% (28/31), respectively.

The sensitivity for identifying genotype-positive LQT2 patients among the LQT2 and Control groups was relatively high under baseline conditions; 83% (19/23), 83% (19/23), and 96% (22/23), respectively. The sensitivity was further improved at steady-state epinephrine effect to 91% (21/23), 91% (21/23), and 96% (22/23), respectively, without the expense of specificity (100% [30/30]).

The sensitivity for identifying genotype-positive LQT3 patients among the LQT3 and Control groups under baseline conditions was 83% (5/6), 50% (3/6), and 100% (6/6), respectively, which was unchanged at steady-state epinephrine effect by any of the three criteria.

Prediction of genotype with epinephrine test

Table 2 illustrates the predictive values with the epinephrine test for genotyping in the prospective study. The Δ mean corrected Q-Tend ≥35 ms at steady-state epinephrine effect could differentiate LQT1 from the LQT2, LQT3, or Control group with predictive accuracy ≥90%. The Δ mean corrected Q-Tend ≥80 ms at peak epinephrine effect could differentiate LQT2 from LQT3 or Control group with predictive accuracy of 100%. Even if we calculated the predictive values by the Δ corrected Q-Tend, which was measured simply from ECG lead V_5, the predictive accuracy still was high (≥80%).

At molecular screening, the responsible mutations could be identified in the first targeted gene suspected by the epinephrine test in all of the 12 LQT1, 12 LQT2, and 3 LQT3 families of the prospective study.

Response to epinephrine test in genotype-unknown patients

Figure 6 illustrates Δ mean corrected Q-Tend at peak (Figure 6A) and steady-state (Figure 6B) epinephrine effects in the 29 patients (15 probands and 14 family members) of the prospective study in whom the responsible mutations could not be identified in any LQTS genes. Among the 15 probands, the response to the epinephrine test was LQT1 pattern in 11 probands and LQT2 pattern in 4 probands. Among the 14 family members, the response was LQT1 pattern in 3 members, LQT2 pattern in 3 members, and LQT3 or Control pattern in 8 members. Even though these 29 patients without causative mutations were included in the analysis for genotype prediction, the positive predictive values were 67% (30/31+14) for LQT1 syndrome and 73% (22/23+7) for LQT2 syndrome, respectively.

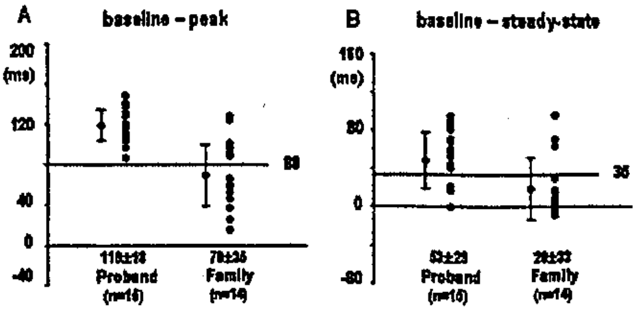

Figure 6 Composite data of changes (Δ) in the mean corrected Q-Tend between baseline conditions and peak epinephrine effects (A) and between baseline conditions and steady-state epinephrine effects (B) in the 29 patients (15 probands and 14 family members) of the prospective study in whom the responsible mutations could not be identified in any LQTS genes.

Complications

Spontaneously terminating torsades de pointes was induced by epinephrine infusion in one LQT1 patient, and spontaneous premature ventricular contractions were induced in one LQT1 and two LQT2 patients.

Discussion

The main findings of the present study are as follows: (1) penetrance in the absence of sympathetic stimulation was lower in LQT1 than in LQT2 or LQT3 syndrome and was improved with steady-state epinephrine in LQT1 and LQT2, but not in LQT3 syndromes; and (2) epinephrine infusion was a powerful test to predict the genotype of LQT1, LQT2, and LQT3 syndromes by comparing the Δ corrected Q-Tend at peak and steady-state epinephrine effects.

Penetrance in LQT1, LQT2, and LQT3 syndromes

It has long been expected that all genotype-positive patients could not be diagnosed by using ECG diagnostic criteria.[17,18] Priori et al[19] conducted molecular screening in nine families with sporadic cases of LQTS and suggested that clinical diagnostic criteria had low sensitivity (penetrance; 38%) in identifying mutation carriers. Swan et al[20] reported that the sensitivity and specificity for identifying genotype-positive patients were 53 and 100%, respectively, in a LQT1 family (D188N). Similarly, in the 12 LQT1 families of the prospective study, the sensitivity for identifying LQT1 patients was low under baseline conditions and was substantially improved with the epinephrine test without the expense of specificity. In contrast, the sensitivity for identifying LQT2 and LQT3 patients was relatively high under baseline conditions in the 12 LQT2 and 3 LQT3 families. These findings suggest the need for molecular screening of all family members regardless of clinical diagnosis to confirm genotype-positive patients, especially in LQT1 syndrome.

Epinephrine test for predicting genotype of LQT1, LQT2, and LQT3 syndromes

Recent clinical data on genotype-phenotype correlation and experimental data in LQTS models have demonstrated the genotype-specific response to sympathetic stimulation and the possibility of genotype-specific therapy.[5–8,11–14,21–23] The LQT1, LQT2, and LQT3 syndromes constitute approximately two thirds of genotyped LQTS patients.[24] Therefore, genotyping of the three forms as well as identifying latent genotype-positive patients are of particular importance in the management and treatment of LQTS patients. Because molecular diagnosis still is unavailable to many institutes, is costly, and is time consuming, genotype identification by clinical tests would be useful for stratifying molecular screening by targeting suspected genes for an initial study.[25–28] Moreover, there are still 30% to 40% of patients clinically affected with LQTS in whom no responsible mutations can be identified. Therefore, it is of great importance to diagnose, based on clinical findings, the form of LQTS that patients are affected with.

Our data demonstrate that epinephrine infusion enables us to predict the genotype of LQT1, LQT2, and LQT3 syndromes as well as to improve the clinical diagnosis of genotype-positive patients, especially in LQT1 syndrome. Genotype prediction of the three syndromes by the epinephrine test would facilitate molecular screening by targeting suspected genes. In fact, molecular screening identified the responsible mutations in the first targeted gene suspected by the epinephrine test in all of the 12 LQT1, 12 LQT2, and 3 LQT3 families of the prospective study. On the other hand, the other 15 probands were assigned to a likely genotype by the epinephrine test, but no mutations were found in any LQTS genes. Because the response to the epinephrine test was LQT1 (11 probands and 3 family members) or LQT2 pattern (4 probands and 3 family members), some ion channel or membrane adapter genes, which are sensitive to catecholamines, may be candidates for responsible genes. It is noteworthy that the positive predictive values for LQT1 and LQT2 syndromes still were high (67% for LQT1 and 73% for LQT2), even though the 29 patients without responsible mutations in any LQTS genes were included in the analysis for genotype prediction. The genotype prediction also may help to stratify the management and treatment of LQTS patients, if the patients cannot be genotyped by the molecular screening.

Conclusion

Epinephrine infusion is a powerful test to predict the genotype of LQT1, LQT2, and LQT3 syndromes as well as to improve the clinical diagnosis of genotype-positive patients, especially in LQT1 syndrome.

Acknowledgments

The authors gratefully acknowledge the expert technical assistance of Ritsuko Yamamoto, Toshiko Shibata, and Naotaka Ohta, Laboratory of Molecular Genetics, National Cardiovascular Center.

References

1. Schwartz PJ, Periti M, Malliani A. The long QT syndrome. Am Heart J 1975;89:378–390.
2. Moss AJ, Schwartz PJ, Crampton RS, Locati E, Carleen E. The long QT syndrome: a prospective international study. Circulation 1985;71:17–21.